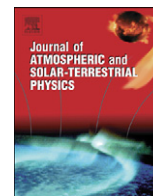




ELSEVIER

Contents lists available at ScienceDirect

## Journal of Atmospheric and Solar-Terrestrial Physics

journal homepage: [www.elsevier.com/locate/jastp](http://www.elsevier.com/locate/jastp)Cosmogenic  $^7\text{Be}$  in air: A complex mixture of production and transportA.-P. Leppänen<sup>a,\*</sup>, A.A. Pacini<sup>b,e,h</sup>, I.G. Usoskin<sup>c</sup>, A. Aldahan<sup>d,j</sup>, E. Echer<sup>b</sup>, H. Evangelista<sup>e</sup>, S. Klemola<sup>f</sup>, G.A. Kovaltsov<sup>g</sup>, K. Mursula<sup>h</sup>, G. Possnert<sup>i</sup><sup>a</sup> Regional Laboratory in Northern Finland, Radiation and Nuclear Safety Authority, Lähteentie 2, 96400 Rovaniemi, Finland<sup>b</sup> National Institute for Space Research (INPE), São José dos Campos, Brazil<sup>c</sup> Sodankylä Geophysical Observatory, University of Oulu, Oulu, Finland<sup>d</sup> Institute of Earth Sciences, University of Uppsala, Sweden<sup>e</sup> University of Rio de Janeiro State, Rio de Janeiro, Brazil<sup>f</sup> Radionuclide Analytics, Radiation and Nuclear Safety Authority, Helsinki, Finland<sup>g</sup> Ioffe Physical-Technical Institute, St. Petersburg, Russia<sup>h</sup> Department of Physics, University of Oulu, Oulu, Finland<sup>i</sup> Tandem Laboratory, University of Uppsala, Uppsala, Sweden<sup>j</sup> Department of Geology, United Arab Emirates University, Al Ain, United Arab Emirates

## ARTICLE INFO

## Article history:

Received 1 April 2010

Received in revised form

8 June 2010

Accepted 8 June 2010

Available online 15 June 2010

## Keywords:

Cosmogenic isotopes

Cosmic rays

Atmosphere

 $^7\text{Be}$ 

NAO

SAM

## ABSTRACT

The long-time series of  $^7\text{Be}$  activity in surface air have been studied with the wavelet analysis technique in order to find coherence between  $^7\text{Be}$  activity, theoretical production in the troposphere and climatic indices. The  $^7\text{Be}$  activity were obtained from five different locations, Angra in the tropics in Brazil, Skåne in mid-latitudes in Southern Sweden, Kiruna in Polar region in Northern Sweden, Loviisa in Southern Finland and Rovaniemi in polar region in Northern Finland. The  $^7\text{Be}$  data from the Northern hemisphere sites were tested for coherence with theoretical production of the isotope in troposphere and with the North Atlantic Oscillation index. In the Southern hemisphere separate theoretical production was calculated in order to describe local production and Southern Annular Mode was used as the climatic index. Consistent and significant coherence were found with theoretical production at Skåne, Kiruna and Loviisa at time-scales of four years or longer. At Angra and Rovaniemi sites, no coherence was detected between  $^7\text{Be}$  theoretical tropospheric production and measured activity at ground level. The coherence between  $^7\text{Be}$  data from Skåne and Angra and climatic indices is insignificant while data from Northern and Eastern Scandinavia show clear coherence with climatic indices at time-scales of four years or longer. Additionally, significant coherence was found between the cosmic ray induced production and NAO at the time band of 8–12 years whereas the coherence between cosmic ray induced production and SAM was insignificant. This feature implies that the ground level  $^7\text{Be}$  activity contain mixed information on both production and transport. This conclusion means that further evaluation through models which enable accurate realistic models that will be investigated in future studies.

© 2010 Elsevier Ltd. All rights reserved.

## 1. Introduction

Cosmogenic nuclides of beryllium are produced in the process of spallation of nitrogen and oxygen nuclei of atmospheric molecules by components of an atmospheric cascade induced by galactic cosmic rays (GCR). Cosmogenic nuclides have been used in many applications ranging from paleoclimatology to solar activity reconstructions. The cosmogenic isotope  $^7\text{Be}$  (half-life of 53.3 days) proved to be useful tracer for atmospheric dynamics. After formation in the atmosphere beryllium is adsorbed on predominantly small sub-micron size aerosols and is transported to ground level via atmospheric vertical mixing (Papastefanou

and Ioannidou, 1995; Winkler et al., 1998). Accordingly,  $^7\text{Be}$  has been proposed as a natural atmospheric tracer (Lal and Peters, 1962; Brost et al., 1991; Vecchi and Valli, 1997). The flux of GCR near the Earth is modulated by the solar magnetic activity. As a result, more cosmic rays are expected around solar minima and vice versa (e.g., Forbush, 1954; Parker, 1965; Vainio et al., 2009). In addition, GCR are moderated by the geomagnetic field and the production of the isotope is therefore higher at higher latitudes. Due to the development of the cosmic-ray induced atmospheric cascade, the  $^7\text{Be}$  production is maximum in the lower stratosphere (around 20 km altitude) and decreases on moving downwards (e.g., Lal and Peters, 1967). Therefore, temporal variations in atmospheric  $^7\text{Be}$  measured near the surface is a potentially tracer of tropospheric dynamics, stratosphere-troposphere coupling and cosmic ray flux variations due to solar activity. Many studies have found connections between solar activity and the  $^7\text{Be}$

\* Corresponding author. Tel.: +358 40 7641788.

E-mail address: [ari.leppanen@stuk.fi](mailto:ari.leppanen@stuk.fi) (A.-P. Leppänen).

concentration in the near-surface air (e.g. Azahra et al., 2003; Talpos et al., 2005; Yoshimori, 2005; Aldahan et al., 2008; Doering and Akber, 2008; Kikuchi et al., 2009). On the other hand, connections between air mass transport and ground level  $^7\text{Be}$  concentration have also been identified, such as seasonal variations caused by stratosphere-troposphere exchange (STE), vertical air mass transport and transport from mid-latitudes to polar regions (Feely et al., 1989; Aldahan et al., 2001; Usoskin et al., 2009a). The surface air  $^7\text{Be}$  activity in the Northern hemisphere reaches its maximum at middle latitudes  $30^\circ\text{N}$ – $40^\circ\text{N}$ , being nearly double that in the polar region (Kulan et al., 2006). Although, surface air  $^7\text{Be}$  activity and factors affecting  $^7\text{Be}$  seasonal variations have been studied widely, studies on  $^7\text{Be}$  inter-annual variations in a full range of both solar and atmospheric changes are scarce.

We note that the modern day climatic studies are largely based upon general circulation models (GCM), which are difficult to test in the atmospheric dynamics (see, e.g., the Fourth Assessment Report of the Intergovernmental Panel on Climate Change at <http://www.ipcc.ch/ipccreports/ar4-wg1.htm>). Owing to recent advances in theoretical studies  $^7\text{Be}$  has become a natural tracer for large scale air mass dynamics, the validity of which on a synoptic time scale was recently demonstrated by Usoskin et al. (2009a). However, before  $^7\text{Be}$  can be fully utilized as a quantitative atmospheric tracer, the seasonal and interannual variations in surface air  $^7\text{Be}$  concentrations must be properly understood.

Countries having nuclear power as a form of energy production routinely monitor radioactivities in ambient air within the framework of radiation protection. As a result,  $^7\text{Be}$  is routinely monitored in many countries around the world. Long-time monitoring of  $^7\text{Be}$  activity data from Brazil and Fennoscandia (Sweden and Finland) were used in this study. The  $^7\text{Be}$  data was analyzed using novel time-series analysis tools and compared against theoretical production in the upper troposphere and climatic indices in order to study the factors influencing  $^7\text{Be}$  activity in ambient air at ground level.

This study was aimed at utilizing  $^7\text{Be}$  as a proxy archive of factors affecting climate such as solar cycle, as well as major teleconnection indices in northern and southern hemisphere.

## 2. Data and analysis

### 2.1. Data sets

Here we analyze the relationships between the following data sets, listed in Table 1. In this study the volumetric activity concentration ( $\text{Bq}/\text{m}^3$ ), the unit in which radioisotope concentrations in air are typically expressed in, has been

denoted as “activity”. First we considered data on  $^7\text{Be}$  activity measured in the near ground air at five low-altitude sites located in far-separated regions of Fennoscandia in Sweden and in Finland, and the southeast-coastal region of tropical Brazil. It should be noted that these sites are located in different climatic zones. The Brazilian site is located at low-latitudes between tropical Hadley cell and mid-latitude Ferrel cell while the Skåne site is located at mid-latitudes inside the Ferrel cell, and the Loviisa site between Ferrel and Polar cells. The two most northern sites, Kiruna and Rovaniemi, are clearly located at high northern latitudes inside the Polar cell.

The atmospheric  $^7\text{Be}$  activity are routinely measured in the framework of radiation safety monitoring in many regions and sites around the globe. The measurements are typically performed in the following way (see details in Mathews and Schulze, 2001; Medici, 2001; Usoskin et al., 2009a). First, ambient air is continuously pumped through a fine fiber-glass filter. At the end of the collection period, which was one week for the Skåne, Kiruna and Rovaniemi sites and two weeks for the Loviisa site, the filters are removed. The usual filter sample treatment method is either to burn or compress the weekly collected filters into a “puck”. In the case of Angra samples, however, the weekly changed filters were collected together during a three-month period and then together placed directly into the detector. The  $^7\text{Be}$  activity is measured with an HPGe gamma-detector mounted inside a lead castle for the reduction of background radiation. The intensity of the 477.59 keV  $\gamma$ -line, corresponding to the decay of  $^7\text{Be}$ , is determined from the measured spectrum. The measured  $^7\text{Be}$  activity is expressed in  $\text{Bq}/\text{m}^3$  (number of disintegration of  $^7\text{Be}/\text{s}/\text{m}^3$  of ambient air). The overall uncertainty of the measurements is typically 7–8% (Usoskin et al., 2009a). The measured activity for all the sites is shown in Fig. 1.

In addition, we have also computed the expected production of  $^7\text{Be}$  by cosmic rays, by means of the CRAC:7Be (Cosmic Ray induced Atmospheric Cascade in application to  $^7\text{Be}$ ) numerical model (Usoskin and Kovaltsov, 2008). We note that the CRAC model for cosmogenic beryllium isotope production agrees with the available experimental data (Usoskin and Kovaltsov, 2008; Usoskin et al., 2009a; Kovaltsov and Usoskin, 2010). It was possible to perform detailed computations on the measurements made since 1951, using the cosmic ray modulation data (Usoskin et al., 2005) and a realistic time-dependent geomagnetic field model IGRF (the International Geomagnetic Reference Field—[http://www.iugg.org/IAGA/iaga\\_pages/pubs\\_prods/igrf.htm](http://www.iugg.org/IAGA/iaga_pages/pubs_prods/igrf.htm)). As an example,  $^7\text{Be}$  production in the polar troposphere (applicable to the Kiruna and Rovaniemi data sets) is shown in Fig. 2A. Similarly we have computed the tropospheric  $^7\text{Be}$  production, denoted as  $Q$  henceforth, for each site.

We also considered two indices of the large-scale atmospheric circulation in the analyzed regions. The large-scale air transport in Northern Europe is largely affected by the NAO (North Atlantic

**Table 1**

Data sets used in this study:  $^7\text{Be}$  activity concentrations measured in near surface air in different sites, computed  $^7\text{Be}$  production as well as two climate mode indices.

Data set	Type	Region	Duration	Geomagnetic cutoff rigidity
Skåne (Swe)	$^7\text{Be}$ activity	56.08°N, 13.23°E	1975–2009	1.9 GV
Kiruna (Swe)	$^7\text{Be}$ activity	67.84°N, 20.34°E	1975–2009	0.5 GV
Loviisa (Fin)	$^7\text{Be}$ activity	60.46°N, 26.23°E	1980–2009	1.4 GV
Rovaniemi (Fin)	$^7\text{Be}$ activity	66.51°N, 25.73°E	1987–2009	0.7 GV
Angra (Bra)	$^7\text{Be}$ activity	23.0°S, 44.32°W	1987–2009	11.6 GV
$Q$	$^7\text{Be}$ production	Computed locally	1951–2009	
NAO	Climate index	North Atlantic	1950–2009	
SAM	Climate index	South mid-high latitudes	1950–2009	

For details see text.

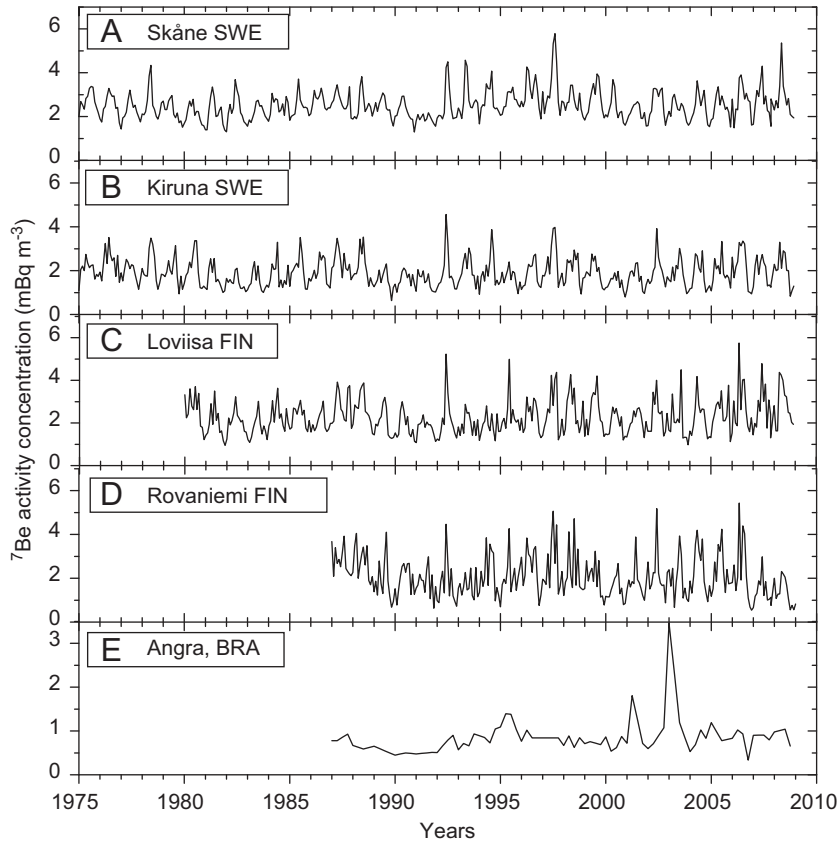


**Fig. 1.** Data on  $^7\text{Be}$  activity measured at near ground air at five sites analyzed here (see Table 1). Data for the Swedish and Finnish sites are monthly averaged while Angra data are 3-month averages.

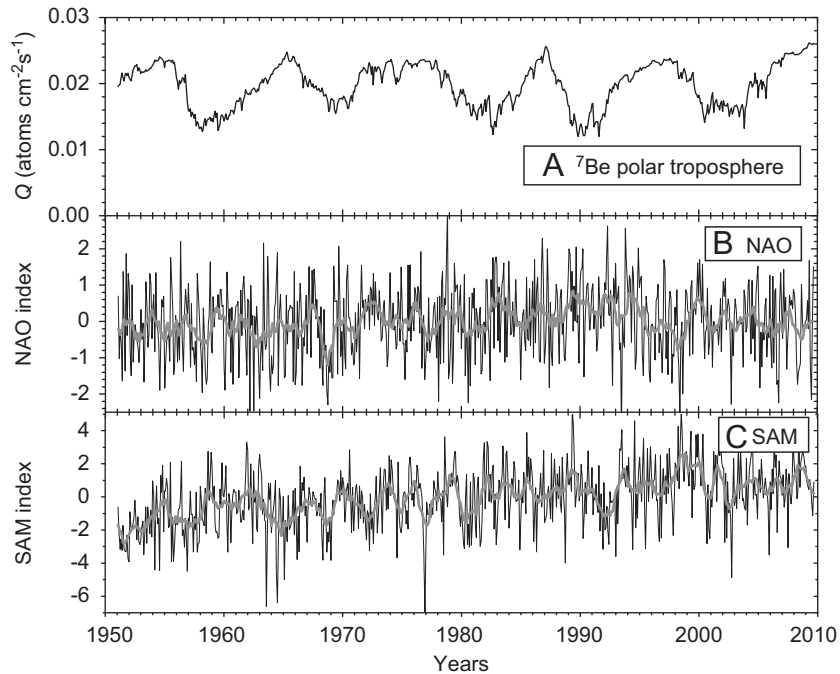


**Fig. 2.** Three external indices discussed here for the period since 1951: Production rate of cosmogenic  $^7\text{Be}$  in the polar troposphere (panel A); North Atlantic Oscillation (NAO) index (panel B); South Annular Mode (SAM) index (panel C). All data are monthly averages, while thick gray curves depict the running annual averages.

Oscillation) index which is defined as the difference in atmospheric pressure at sea-level between the Icelandic low and the Azores high. The data set was obtained from the National Oceanic

and Atmospheric Administration (NOAA) National Weather Service Climate Prediction Center (<http://www.cpc.ncep.noaa.gov/data/teledoc/nao.shtml>).

Another index was chosen for the Southern hemisphere large scale circulation, SAM (Southern Annular Mode index also referred as Antarctic Oscillation, AAO), which is defined as the difference in the normalized monthly zonal-mean sea level pressure between 40°S and 70°S (Nan and Li, 2003). The data set was obtained from [http://www.lasg.ac.cn/staff/ljp/data-NAM-SAM-NAO/SAM\(AAO\).htm](http://www.lasg.ac.cn/staff/ljp/data-NAM-SAM-NAO/SAM(AAO).htm). SAM is dominant pattern of non-seasonal tropospheric circulation variations south of 20S. The <sup>7</sup>Be concentrations reach maximum at mid-latitudes and it is transported to higher and lower latitudes (Kulan et al., 2006). SAM affects the climate patterns in latitudinal direction while ENSO/SOI effects mainly in longitudinal direction. As mentioned previously, <sup>7</sup>Be is an indicator of vertical tropospheric circulation. The influence of SAM is probable at Angra site since Angra is located close to the edge of the area of influence of SAM.

Since we were interested in long-term (inter-annual) relationships, we have used monthly averaged data in all cases except for the Angra <sup>7</sup>Be activity, which was originally 3-month averaged.

## 2.2. Analysis method

First we computed the traditional bivariate Pearson's correlation between the series. This quantifies in one number the overall correlation between the two entire series on all time scales. The correlation coefficients are given in Table 2 for all the analyzed series. One can see that measured <sup>7</sup>Be activity is significantly correlated with the production *Q* in Skåne, Kiruna and Loviisa, and marginally significant correlation in Rovaniemi and non-significant correlation in the Angra sites. On the other hand, the correlation between <sup>7</sup>Be activity concentration and NAO/SAM is formally significant only for the Finnish sites. The different indices did not show any meaningful correlation between each other. The correlation is weak (explaining less than 10% of the data variability) in all cases.

However, correlation coefficients alone do not allow study of the details of the relationships between the series. For instance, it does not properly consider the possible phase difference between the series, nor does it take into account possible strengthening or weakening of the coherence. Moreover, the ambient air <sup>7</sup>Be activity can be largely affected by the seasonal variability, especially by Spring and/or Autumn stratospheric-tropospheric mixing (Aldahan et al., 2008). Accordingly, in the next step we consider the wavelet coherence between series *x* and *y*, that is defined as the normalized wavelet cross-spectrum

$$WC_{xy}(f,t) = \frac{|W_{xy}(f,t)|^2}{W_{xx}(f,t) \cdot W_{yy}(f,t)}, \quad (1)$$

where *W* stands for the wavelet spectral density localized at frequency *f* and time *t* (Torrence and Compo, 1998). Wavelet coherence determines both the absolute magnitude, defined between 0 (no coherence) and 1 (100% coherence), and the phase shift between the series, as a function of the frequency/time scale and time. The wavelet coherence can be regarded as localization of the correlation in the time and frequency domains, and reveals the locations in both time and frequency where the coherence is large. Here we applied the standard Morlet basis for the wavelet spectra with the damping parameter (or dimensionless time—see

Grinsted et al., 2004) *k*=3, which provides an optimal time resolution (in particular reducing the cone of influence) at the cost of lower frequency resolution. We note that, for the selected parameters, the time scale (i.e., effective expansion of a wavelet package in the time domain) is close to the nominal Fourier period (i.e., inverted carrier frequency of the Morlet function). Therefore, we use the term “time scale” throughout the paper.

The obtained wavelet coherence as function of time and frequency are shown in Figs. 3 and 4. The magnitude of the coherence is given in color, from blue for 0 to red for 1. Regions with highly significant coherence (> 95%) are bound by the solid black lines. The statistical significance of the wavelet coherence was estimated using the non-parametric random phase test (Kumar and Foufoula-Georgiou, 1994; Ebisuzaki, 1997; Usoskin et al., 2009b). The local phase between the series is depicted by arrows. Arrows pointing horizontally right, horizontally left, down or up imply that the wavelets of the compared series at a given frequency and time are exactly in phase, in anti-phase, or series *y* is leading or lagging by a quarter of the period, respectively. Thick white curves denote the cone of influence (COI), which indicate that the results can be affected by the edges of the series and thus are not reliable outside these limits. Here the COI is defined as the area in which the wavelet power caused by the discontinuity at the edge drops to *e*<sup>-2</sup> of the value at the edge (Grinsted et al., 2004). Thus, strictly speaking, the areas outside the COI need to be omitted.

## 2.3. Analysis of data

First we compared the external indices data sets, as shown in Fig. 3. Panel A shows the coherence between the <sup>7</sup>Be production term, *Q*, (in the polar troposphere) and the NAO index. Simple correlation (Table 2) suggests a very weak and insignificant inverted relationship between the *Q* and NAO indices, but the coherence plot shows much more detail. One can see that there is no coherent variability of the two series at the inter-annual time scale shorter than 8 years, but there is a highly significant strong (0.7–0.8) coherence at the 8–12 year time band.

The phase of the coherence is about 180°, corresponding to the inverted relationship between the series. However, this strong coherence exists only after 1985 with no relationship prior to that year (there is a hint of a similar relationship appearing again before 1955, but this is not within COI). We note that such an intermittent relationship between different solar indices and NAO is in agreement with some earlier findings (e.g. Thejll et al., 2003; Huth et al., 2006; Georgieva et al., 2007; Zanchettin et al., 2008). However, we cannot conclude in the framework of this study whether this intermittent relation is a real link or a coincidence of two independent variable signals with similar period.

Panel B of Fig. 3 shows the coherence between *Q* and SAM indices, which depict no mutual relation from the simple correlation analysis. In fact, no systematic coherence was observed for the time scale shorter than 8 years. Furthermore, there is strong intermittent coherence between the series at the time band of 8–12 years, before 1970 and after 1990. However, a more detailed examination suggests that the phase of the

**Table 2**

Bivariate correlation coefficients for all the analyzed series with the polar <sup>7</sup>Be production and NAO indices, together with the 68% confidence level (one standard deviation).

	Skåne	Kiruna	Loviisa	Rovaniemi	Angra	SAM	NAO
<i>Q</i>	0.29 ± 0.09	0.31 ± 0.05	0.26 ± 0.05	0.12 ± 0.06	0.11 ± 0.10	0 ± 0.04	-0.07 ± 0.03
NAO <sup>a</sup>	-0.11 ± 0.05	-0.04 ± 0.05	-0.17 ± 0.05	-0.15 ± 0.06	0.05 ± 0.10	0.08 ± 0.03	N/A

<sup>a</sup> For Angra, the SAM, not NAO, index was used.

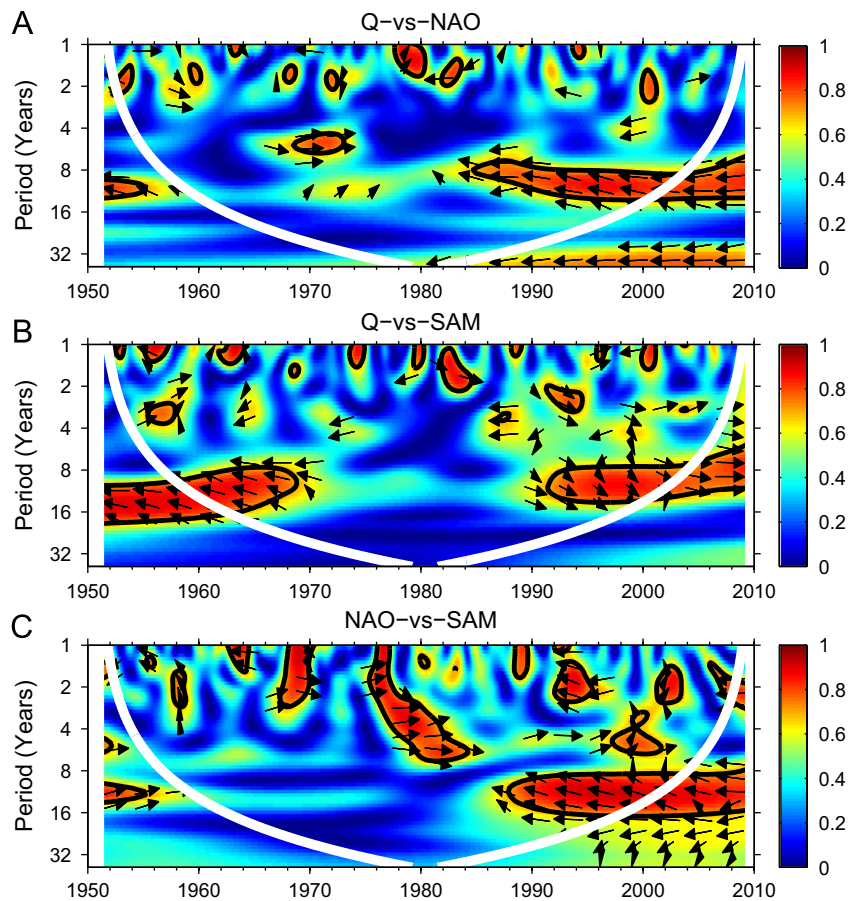


**Fig. 3.** Plots of the wavelet coherence between pairs of the studied external indices, as denoted on top of each panel. Coherence magnitude is given in color (see color scale on the right), and phase indicated by arrows. Thick white curve depicts the cone of influence (COI). (For interpretation of the references to color in this figure legend, the reader is referred to the web version of this article.)

relationship is not consistent—it slowly changes from about  $45^\circ$  ca. 1990 to  $0^\circ$  after 2000, and, is about  $-150^\circ$  before 1970. This feature provides a clear sign of a casual relationship, like combating of independent signals with close periodicities.

The relationship between the SAM and NAO indices (Fig. 3C) shows no systematic coherence except for the time band of 8–12 years after 1990, when the two series are essentially coherent with a relative phase of about  $-150^\circ$ .

Thus, all the three indices, Q, NAO and SAM, show coherence only at the time band of 8–12 years after the late 1980s, implying that all the indices show similar variability during that period. This behavior is likely to be a casual relationship attributable to similar variability modes.

Next we compared the measured  $^7\text{Be}$  activity with the external indices, as depicted in Fig. 4. Here we analyzed the coherence of all the data series for individual sites with the local production Q and the dominant climate mode, NAO for the Fennoscandian sites and SAM for the Brazilian site.

The mid-latitude Swedish site (Skåne) demonstrates high coherence between the data and production rate on a time scale longer than six years (Fig. 4A1). The relative phase has no shift, which implies that the variations in the measured  $^7\text{Be}$  activity are in fact determined by its atmospheric production. There is a significant inverted relationship between the measured activity and the NAO index (Fig. 4A2) after 1990. Another Swedish site, polar Kiruna, shows a similar behavior with a strong production signal at a time scale longer than six years (Fig. 4B1) and a somewhat weaker NAO inverted signal after 1990 (Fig. 4B2). The latter can be due to the existing coherence between NAO and Q

with inverted phase (Fig. 3A). Furthermore, there is no dominant signal at the time scale shorter than 5–6 years. A somewhat similar result was found at the Loviisa site in Southern Finland—a strong production signal (Fig. 4C1) and significant coherence with the NAO variations (Fig. 4C2).

However, the situation at the polar Finnish site Rovaniemi is relatively different. While the production signal is nearly absent (Fig. 4D1), the NAO signal is relatively visible before 2001 (Fig. 4D2), at time scale longer than four years. Even though the time series is shorter for Rovaniemi, it seems that NAO dominates the activity of the isotope at this site, and not the production. In addition, the Rovaniemi data were tested for coherence with the Arctic Oscillation (AO) but no coherence was found.

In Finland southwestern winds that transport maritime air from the Atlantic region are common. These winds generally carry low concentrations of  $^7\text{Be}$ , partly due to significant wet and dry deposition in the North Atlantic along the path of the Gulf stream. According to Field et al. (2006), there is less deposition of beryllium in the Arctic region, and lowest amount in continental regions, compared to the path of Gulf stream in the North Atlantic. It should be noted that Field et al. (2006) has calculated wet and dry deposition for  $^{10}\text{Be}$ , but not for  $^7\text{Be}$ . However, the  $^7\text{Be}$  is attached to sub-micron size accumulation mode aerosol particles (Winkler et al., 1998). When attached to relatively heavy aerosol the mass difference of different beryllium isotopes only accounts for few percent of the mass of the whole aerosol. The only significant difference is the decay rates which may produce difference in  $^{10}\text{Be}$  and  $^7\text{Be}$  deposition. Despite this,  $^{10}\text{Be}$  deposition maps are used in this study to estimate  $^7\text{Be}$  deposition.

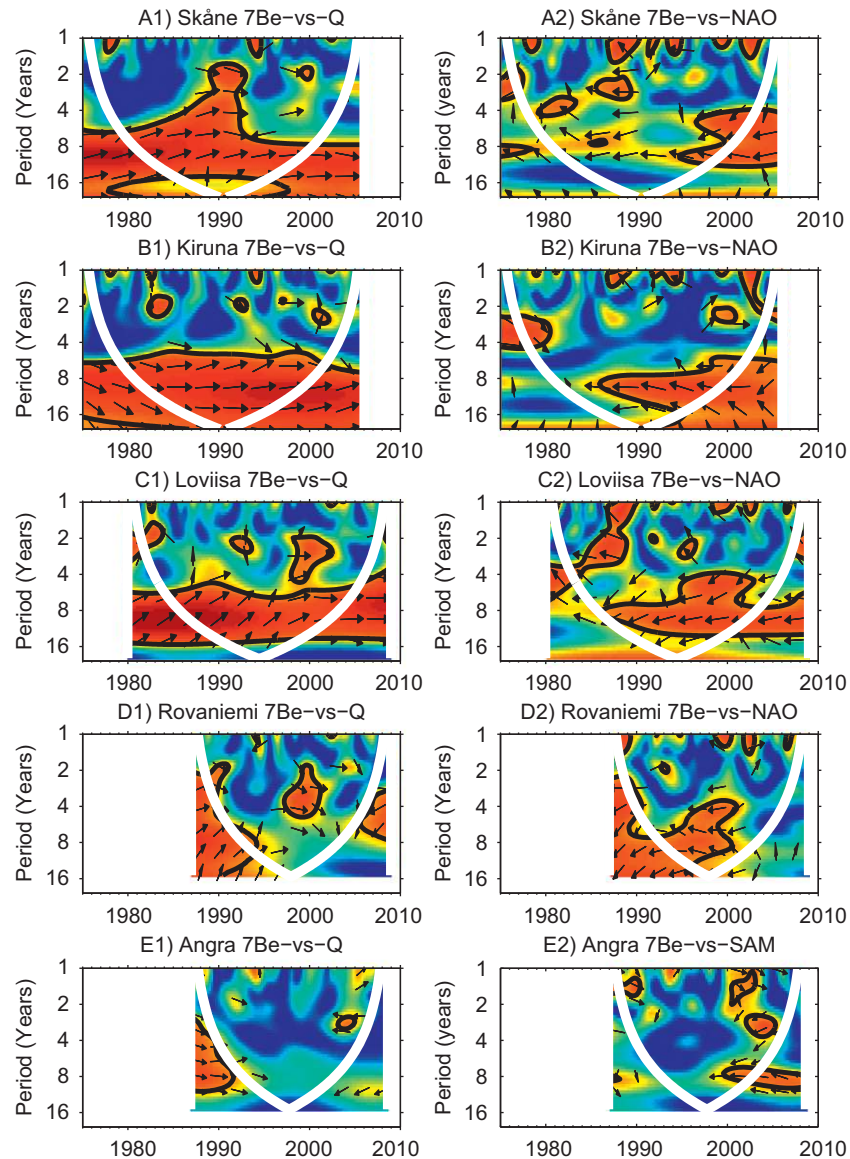


**Fig. 4.** Similar to Fig. 3 but for  $^7\text{Be}$  data vs. external indices. (For interpretation of the references to color in this figure legend, the reader is referred to the web version of this article.)

Judging from the available data (Figs. 1, 2 and 4) there is no clear reason or explanation for the intermittent coherence between  $^7\text{Be}$  and NAO signal. For example, the 8 year periodicity does not become significant in Kiruna data until 1993, although there are indications of 8 year periodicity around 1985. Interestingly, the coherence in Rovaniemi data seems to work almost in opposite phase compared to that of Kiruna data. In Rovaniemi data the 8 year signal is present until 2000. The  $\sim 4$  year NAO period is present in Rovaniemi, Loviisa, Skåne and Kiruna datasets during 1995–2000 when NAO index was dominantly negative. In each case the  $^7\text{Be}$  concentrations are in opposite phase compared to the NAO index. The disappearance of coherence in Rovaniemi data can be a result of strengthening influence of continental air masses in Northern Finland. This in turn could hinder the incoming low-pressures from Atlantic to enter Northern Finland and cause the precipitation to rain in Fennoscandian mountains increasing the influence of NAO in Kiruna region. The coherence between  $^7\text{Be}$  and NAO in lower latitude site in date from Skåne and Loviisa starts around 1986–1987 as a 8 year periodicity. This would suggest that more marine air has entered to Southern parts of Scandinavia starting from 1986 has continued since. The cause

for these phenomena is most likely related to evolution of large scale climatic systems rather than just local climatic evolution in Fennoscandia.

NAO is also known to modulate the concentrations of other radioactive isotopes in ambient air. For example, the  $^{210}\text{Pb}$  concentration in ground level air in Finland is effected by NAO (Paatero et al., 2000). At times with a low NAO index, continental air masses with high  $^{210}\text{Pb}$  concentrations become more frequent. During a high NAO index westerly winds bring maritime air with low  $^{210}\text{Pb}$  concentrations. This relationship is weaker in Northern Finland due to the more frequent occurrence of Arctic air masses. It should be noted that, while  $^7\text{Be}$  is formed in the stratosphere and in the upper troposphere,  $^{210}\text{Pb}$  is a decay product of  $^{222}\text{Rn}$  and is produced at ground level. Similarly to  $^7\text{Be}$ ,  $^{210}\text{Pb}$  has also been used as an atmospheric tracer e.g. see Paatero et al. (1998) and references therein.

A similar pattern, as in Rovaniemi, was observed at the tropical Brazilian site—the total absence of the production signal (Fig. 4E1) and an unsettled possible presence of the climate SAM signal (Fig. 4D2) after 1999. The Angra data were also tested for coherence with Southern Oscillation Index (SOI) but no

coherence was found. For this site, the lack of any production imprints over the  $^7\text{Be}$  data can be understood as a consequence of the high, local geomagnetic cutoff rigidity ( $P_c \approx 12 \text{ GV}$ ). This means that a major part of the  $^7\text{Be}$  activity found at this latitude were not produced locally, but brought by air-masses from other sites with a higher latitude (and thus higher production), leaving the transport and deposition to dominate the variability observed in the data. The atmospheric circulation at this site is mainly from east to west, facilitating the entrance of oceanic air-masses. There are two kinds of oceanic air masses that reach the Brazilian south-east coast: warm air masses composed of a mixture of Atlantic tropical mass and Atlantic equatorial mass; and cold masses represented by Atlantic polar mass. The alternation between cold and warm air masses drives the medium-low latitudes climate (Ross, 2005). This atmospheric circulation pattern is affected by many Southern hemisphere climatic systems, which seem to be partially dependent on the SAM signal (Silvestri and Vera, 2003). Gillett et al. (2006) showed that SAM has significant impacts on temperature and precipitation over different Southern hemisphere areas (not directly on Rio de Janeiro), and this could be associated with changes in the regional wind pattern, explaining the weak relationship found between the  $^7\text{Be}$  activity in Brazilian data and the SAM climate index. Moreover, according to Field et al. (2006), the Angra site belongs to a region of strong dry and wet deposition of beryllium where strong local rainfall most likely smears the coherence patterns. Similarly to Skåne and Kiruna data the coherence with Angra data and SAM index gets stronger beginning from year 2000.

Unfortunately, the latter two data series, Rovaniemi and Angra, are shorter than the others, and COI occupies only part of the coherence map. As a result, the coherence results for these data sets are only relatively indicative but in time when more data have been collected this can possibly be verified conclusively.

Briefly, the observed relationships can be summarized as follows:

- There is significant coherence between NAO and cosmic ray variations after ca. 1985 at the time scale of around 10 years.
- Although there is significant coherence between cosmic ray variations and SAM before 1970 and after 1990, the relative phasing suggests that it is an artefact.
- Coherence between the SAM and NAO indices exists only after 1990.
- There is no coherence between the measured data and any of the driving indices on the time scale shorter than about 5 years.
- The activity of  $^7\text{Be}$  is determined primarily by variations in production in the south and western parts of Fennoscandia.
- The activity of  $^7\text{Be}$  is determined primarily by large scale air dynamics (NAO index) in east-north Fennoscandia.
- The activity of  $^7\text{Be}$  depicts no production signal in the tropical Brazilian site, and is probably marginally affected by the SAM climate index.

### 3. Discussion and conclusions

We have presented an effort to identify the main drivers of the  $^7\text{Be}$  temporal modulation at different geographical locations by comparing the production and the climatic imprints over the data. We used a novel theoretical model (CRAC:7Be—Usoskin and Kovaltsov, 2008) to generate a time series of production of  $^7\text{Be}$  by cosmic rays in the troposphere. Long-term series of observational data of ambient air  $^7\text{Be}$  activity were obtained from

five different sites in Fennoscandia and in Brazil along with the NAO and SAM teleconnection indices. The wavelet coherence method was used to analyze the coherence between the  $^7\text{Be}$  activity and external indices time-series. The analysis shows that the  $^7\text{Be}$  activity in surface air at each site behave uniquely. Each site has its own combination of different factors that affect the surface air  $^7\text{Be}$  activity.

The mid-latitude station at Skåne shows a significant coherence with the production signal from GCRs but not with NAO index. Skåne is mainly influenced by the maritime air from the Atlantic and is located close to mid-latitudes where the  $^7\text{Be}$  concentrations reach maximum values. It is natural that the production signal from Q is strong and dominant. In the north-western part of Scandinavia, the Kiruna region, the  $^7\text{Be}$  activity is mainly affected by both maritime air masses from the Atlantic and by polar air masses from the Arctic. A relationship was also found between the NAO index and  $^7\text{Be}$  activity concentrations was also found in the  $^7\text{Be}$  datasets from eastern and northern Fennoscandia. As a whole, Fennoscandia is located in the transition zone between the North Atlantic region and the continental area of Eurasia. The Northern and Eastern part of Fennoscandia are also affected by polar air masses from the Arctic. The absence of a clear production Q signal in the Rovaniemi data is most likely due to its location at northern high latitude and the climatic nature of the region where air masses from three climatic types mix. This, in turn, can also explain the presence of the NAO signal in which air masses from the Atlantic have a strong effect on the climate in Rovaniemi. The Loviisa site is located in Southern Finland, where air currents bring  $^7\text{Be}$ -rich air from mid-latitudes which, in turn, can explain the presence of the Q signal in the data. Like Rovaniemi, Loviisa is also located in the transition zone between the North Atlantic region and the Eurasian continent which can explain the presence of NAO in the  $^7\text{Be}$  data. Compared to Rovaniemi, less Arctic air masses reach the Loviisa site.

In the southern hemisphere at Angra, local climatic systems are responsible for the strong atmospheric mixing and strong scavenging effects, implying the absence of dominant signals from both Q and SAM in the  $^7\text{Be}$  data.

In conclusion, we found a geographically dependent response to variations in  $^7\text{Be}$  production, as well as a strong imprint of the local climatic pattern, identified in  $^7\text{Be}$  data. Although, no clear unified separation of the production and transport signals can be made for the  $^7\text{Be}$  data, recent models make it possible to study both effects. This implies that atmospheric  $^7\text{Be}$  sampled in near-surface air has great potential as a useful tracer of the large-scale air mass dynamics.

### Acknowledgments

We would like to acknowledge the work of John C. Moore and Aslak Grinsted of the University of Lapland and Svetlana Jevrejeva of the Proudman Oceanographic Laboratory for making the wavelet coherence software package used in this work and making it available at [http://www.pol.ac.uk/home/research/wavelet\\_coherence/](http://www.pol.ac.uk/home/research/wavelet_coherence/). The authors thanks the Laboratory of Environmental Monitoring/Eletronuclear in Brazil and Dr. Sergio Ney, for making Angra data available for this work. The Swedish data were measured and kindly provided by the Swedish Defence Research Agency (FOI). AP thanks to CNPq and CIMO for the financial support. EE thanks CNPq (PQ 300211/2008-2) and FAPESP (2007/52533-1) agencies for financial support. GAK was partly supported by the Program of Presidium RAS N16-3-5.4. Support from the Academy of Finland is also acknowledged.

## References

- Aldahan, A., Hedfors, J., Possnert, G., Kulan, A., Berggren, A., Söderström, C., 2008. Atmospheric impact on beryllium isotopes as solar activity proxy. *Geophys. Res. Lett.* 35, L21812.
- Aldahan, A., Possnert, G., Vintersved, I., 2001. Atmospheric interactions at northern high-latitudes from weekly Be-isotopes in surface air. *Appl. Radiat. Isotop.* 54, 345–353.
- Azahra, M., Camacho-García, A., González-Gómez, C., López-Peñalver, J., El Bardouni, T., 2003. Seasonal <sup>7</sup>Be concentrations in near-surface air of Granada (Spain) in the period 1993–2001. *Appl. Radiat. Isotop.* 59, 159–164.
- Brost, R.A., Feichter, J., Heimann, M., 1991. Three-dimensional simulation of <sup>7</sup>Be in a global climate model. *J. Geophys. Res.* 96, 22423–22445.
- Doering, C., Akber, R., 2008. Beryllium-7 in near-surface air and deposition at Brisbane, Australia. *Australia. J. Environ. Radioact.* 99, 461–467.
- Ebisuzaki, W., 1997. A method to estimate the statistical significance of a correlation when the data are serially correlated. *J. Clim.* 10 (September), 2147–2153.
- Feely, H.W., Larsen, R.J., Sanderson, C.G., 1989. Factors that cause seasonal variations in beryllium-7 concentrations in surface air. *J. Environ. Radioact.* 9, 223–249.
- Field, C., Schmidt, G., Koch, D., Salyk, C., 2006. Modeling production and climate-related impacts on <sup>10</sup>Be concentration in ice cores. *J. Geophys. Res.* 111, D15107.
- Forbush, S., 1954. World-wide cosmic-ray variations, 1937–1952. *J. Geophys. Res.* 59 (4), 525–542.
- Georgieva, K., Kirov, B., Tonev, P., Guineva, V., Atanasov, D., 2007. Long-term variations in the correlation between NAO and solar activity: the importance of north south solar activity asymmetry for atmospheric circulation. *Adv. Space Res.* 40, 1152–1166.
- Gillett, N.P., Kell, T.D., Jones, P.D., 2006. Regional climate impacts of the Southern Annular Mode. *Geophys. Res. Lett.* 33, L23704.
- Grinsted, A., Moore, J.C., Jevrejeva, S., 2004. Application of the cross wavelet transform and wavelet coherence to geophysical time series. *Nonlin. Process. Geophys.* 11, 561–566.
- Huth, R., Pokorná, L., Bochníček, J., Hejda, P., 2006. Solar cycle effects on modes of low-frequency circulation variability. *J. Geophys. Res.* 111, D22107.
- Kikuchi, S., Sakurai, H., Gunji, S., Tokanai, F., 2009. Temporal variation of <sup>7</sup>Be concentrations in atmosphere for 8 y from 2000 at Yamagata, Japan: solar influence on the <sup>7</sup>Be time series. *J. Environ. Radioact.* 100, 515–521.
- Kovaltsov, G.A., Usoskin, I.G., 2010. A new 3D numerical model of cosmogenic nuclide <sup>10</sup>Be production in the atmosphere. *Earth Planet. Sci. Lett.* 291, 182–188.
- Kulan, A., Aldahan, A., Possnert, G., Vintersved, I., 2006. Distribution of <sup>7</sup>Be in surface air of Europe. *Atmos. Environ.* 40, 3855–3868.
- Kumar, P., Foufoula-Georgiou, E., 1994. Introduction to wavelet transforms. In: Foufoula-Georgiou, E., Kumar, P. (Eds.), *Wavelets in Geophysics*. Academic Press.
- Lal, D., Peters, B., 1962. Cosmic ray produced isotopes and their application to problems in geophysics. In: Wilson, J., Wouthuysen, S. (Eds.), *Progress in Elementary Particle and Cosmic Ray Physics*, vol. 6. North-Holland, Amsterdam, pp. 77–243.
- Lal, D., Peters, B., 1967. Cosmic ray produced radioactivity on the earth. In: Sittle, K. (Ed.), *Handbuch der Physik*, vol. 46(2). Springer, Berlin, pp. 551–612.
- Mathews, S., Schulze, J., 2001. The radionuclide monitoring system of the comprehensive-nuclear test ban treaty organisation: from sample to product. *Kerntechnik* 66, 102–112.
- Medici, F., 2001. Particulate sampling in the IMS radionuclide network of the comprehensive-nuclear test ban treaty. *Kerntechnik* 66, 121–125.
- Nan, S., Li, J., 2003. The relationship between the summer precipitation in the Yangtze River valley and the boreal spring Southern Hemisphere annular mode. *Geophys. Res. Lett.* 30 (CiteID 2266).
- Paatero, J., Hatakka, J., Mattson, R., Viisanen, Y., 1998. Analysis of daily <sup>210</sup>Pb air concentrations in Finland, 1967–1996. *Radiat. Prot. Dos.* 77 (3), 191–192.
- Paatero, J., Hatakka, J., Mattsson, R., Aaltonen, V., Viisanen, Y., 2000. Long-term variations of <sup>210</sup>Pb concentrations in ground-level air in Finland: effects of the North Atlantic Oscillation. In: Midgley, P., Reuther, M., Williams, M. (Eds.), *Transport and Chemical Transformation in the Troposphere: Proceedings of the EUROTRAC-2 Symposium 2000*. Springer-Verlag, Berlin, Germany, pp. 322–324.
- Papastefanou, C., Ioannidou, A., 1995. Aerodynamic size association of Be-7 in ambient aerosols. *J. Environ. Radioact.* 26, 273–282.
- Parker, E., 1965. The passage of energetic charged particles through interplanetary space. *Planet. Space Sci.* 13, 9–49.
- Ross, J., 2005. *Geografia do Brasil*, fifth ed. Edusp, Sao Paulo.
- Silvestri, G.E., Vera, C.S., 2003. Antarctic Oscillation signal on precipitation anomalies over southeastern South America. *Geophys. Res. Lett.* 30 (21) (CiteID 2115).
- Talpos, S., Rumbu, N., Borsan, D., 2005. Solar forcing on the <sup>7</sup>Be-air concentration variability at ground level. *J. Atmos. Solar-Terr. Phys.* 67, 1626–1631.
- Thejll, P., Christiansen, B., Gleisner, H., 2003. On correlations between the North Atlantic Oscillation, geopotential heights, and geomagnetic activity. *Geophys. Res. Lett.* 30 (6) (CiteID 1347).
- Torrence, C., Compo, G., 1998. A practical guide to wavelet analysis. *Bull. Am. Meteorol. Soc.* 79, 61–78.
- Usoskin, I., Kovaltsov, G., 2008. Production of cosmogenic <sup>7</sup>Be isotope in the atmosphere: full 3D modelling. *J. Geophys. Res.* 113, D12107.
- Usoskin, I.G., Alanko-Huotari, K., Kovaltsov, G.A., Mursula, K., 2005. Heliospheric modulation of cosmic rays: monthly reconstruction for 1951–2004. *J. Geophys. Res.* 110, A12108.
- Usoskin, I.G., Field, C.V., Schmidt, G.A., Leppänen, A.-P., Aldahan, A., Kovaltsov, G.A., Possnert, G., Ungar, R.K., 2009a. Short-term production and synoptic influences on atmospheric <sup>7</sup>Be concentrations. *J. Geophys. Res.* 114, D06108.
- Usoskin, I.G., Horiuchi, K., Solanki, S., Kovaltsov, G.A., Bard, E., 2009b. On the common solar signal in different cosmogenic isotope data sets. *J. Geophys. Res.* 114, A03112.
- Vainio, R., Desorgher, L., Heynderickx, D., Storini, M., Flückiger, E., Horne, R.B., Kovaltsov, G.A., Kudela, K., Laurenza, M., McKenna-Lawlor, S., Rothkaehl, H., Usoskin, I.G., 2009. Dynamics of the Earth's particle radiation environment. *Space Sci. Rev.* 147, 187–231.
- Vecchi, R., Valli, G., 1997. <sup>7</sup>Be in surface air: a natural atmospheric tracer. *J. Aerosol Sci.* 28 (5), 895–900.
- Winkler, R., Diel, F., Frank, G., Tschiersch, J., 1998. Temporal variation of <sup>7</sup>Be and <sup>210</sup>Pb size distributions in ambient aerosol. *Atmos. Environ.* 32 (6), 983–991.
- Yoshimori, M., 2005. Beryllium 7 radionuclide as a tracer of vertical air mass transport in the troposphere. *Adv. Space Res.* 36, 828–832.
- Zanchettin, D., Rubino, A., Traverso, P., Tomasino, M., 2008. Impact of variations in solar activity on hydrological decadal patterns in northern Italy. *J. Geophys. Res.* 113, D12102.